Accepted for publication in Journal of Applied Polymer Science

Published in February 15, 2013

DOI: 10.1002/app.39004

Essential Work of Fracture (EWF) of Poly(ε-caprolactone)/Boehmite Alumina Nanocomposites: Effect of Surface Coating

by

F. Tuba[1], V. M. Khumalo[2] and J. Karger-Kocsis[1,3*]

[1]Department of Polymer Engineering, Faculty of Mechanical Engineering, Budapest University of Technology and Economics, H-1111 Budapest, Muegyetem rkp. 3., Hungary

[2]Department of Polymer Technology, Faculty of Engineering and Built Environment, Tshwane University of Technology, Pretoria 0001, Republic of South Africa

[3]MTA–BME Research Group for Composite Science and Technology, Muegyetem rkp. 3., H-1111 Budapest, Hungary

* Author to whom correspondence should be addressed,

E-mail: karger@pt.bme.hu

Submitted to J. Appl. Polym. Sci., October, and revised November, 2012

Abstract

The essential work of fracture (EWF) approach has been adopted to reveal the effect of nanofillers on the toughness of poly(ε-caprolactone)/boehmite alumina (PCL/BA) nanocomposites. Synthetic BA particles of different surface treatments were dispersed in the PCL matrix by extrusion melt compounding. The morphology of composites was studied by scanning electron microscopy. Differential scanning calorimetry and wide angle X-ray scattering were used to detect changes in the crystalline structure of PCL. Besides the mode I type EWF tests, dynamic mechanical analysis (DMA) and quasi-static tensile tests were applied to study the effect of BA nanofillers on the mechanical properties. BA was homogenously dispersed and acted as heterogeneous crystallization nucleant and non-reinforcing filler in PCL. The tensile modulus and yield strength slightly increased, whereas the yield strain decreased with increasing BA content (up to 10 wt%). Effect of the BA surface treatment with octylsilane (OS) was negligible by contrast to alkylbenzene sulphonic acid (OS2). Like the tensile mechanical data, the essential and non-essential work of fracture parameters did not change significantly, either. Improved PCL/BA adhesion in case of OS2 treatment excluded the usual EWF treatise. This was circumvented by making use of energy partitioning between yielding and necking. The yielding related essential work of fracture decreased while the non-essential one increased with BA content and with better interfacial adhesion. This was attributed to the effect of matrix/filler debonding.

Key-words: nanocomposites, essential work of fracture (EWF), poly(ε-caprolactone), boehmite, surface coating

1. INTRODUCTION

The essential work of fracture (EWF) approach is gaining acceptance to determine the plane stress toughness of highly ductile polymers in their sheet, film forms [1-4]. According to the EWF, the stable crack growth occurring in the specimen is due to an increasing work input in an inner region being "filtered" through the gradually increasing action of the dissipative work in the neighboring region. Thus the total work of fracture includes both the dissipative work in the outer "plastic" zone and the essential one in the inner zone (cf. Figure 1). The latter is termed to fracture process zone and the related essential work of fracture in plane-stress is a geometry-independent toughness parameter and thus represents a material property. On the other hand, the non-essential or "plastic" work is a geometry-dependent parameter. The attribute "plastic" may suggest that in the outer fracture zone irreversible deformation takes place which is not always the case for polymers.

As written above the total work of fracture (W_f) can be partitioned into two components; i) the essential work of fracture (W_e) consumed in the inner fracture process zone to create new crack surfaces, and ii) the non-essential (or plastic) work (W_p) performed in the outer "plastic" deformation zone – see Figure 1.

Figure 1: Schematic diagram showing the fracture zones in a double edge-notched tensile-loaded (DENT) specimen (a) (FPZ: inner fracture process zone, PDZ: outer plastic dissipative zone) and the data reduction method of the EWF (b). Notes: this figure indicates the usual criteria [3,4] for the minimum and maximum ligament lenths (L_{min} and L_{max}, respectively) of valid plane-stress tests. r_p denotes the radius of the plastic zone.

The total work of fracture (W_f), calculated from the area of the load-displacement (F-x) curves is composed of:

$$W_f = W_e + W_p \tag{1}$$

Assuming that W_e depends on initial cross-section and W_p on the plastic volume (cf. Figure 1a), Equation (1) can be rewritten into specific terms (Equations (2) and (3)):

$$W_f = w_e \cdot Lt + \beta w_p \cdot L^2 t \tag{2}$$

$$w_f = w_e + \beta w_p \cdot L \tag{3}$$

where L is the ligament length, t is the specimen thickness and β is the shape factor related to the form of the outer plastic dissipation zone. In the outer plastic dissipation zone crazing, voiding, shear deformation and their combination may be at work. Recall that w_e is surface-, whereas w_p is volume-related Equation (3) is the base of the data reduction: the specific work of fracture data (w_f), determined on specimens with different ligaments, are plotted as a function of the ligament length. This simple mode of testing is the major reason of the popularity of the EWF. On the other hand, researchers often disregard whether the basic criteria of the EWF application hold or not [4-5]. These criteria are [4]: presence of quasi plane-stress condition (taken into consideration by a "valid" ligament range), full ligament yielding of the specimens prior to crack growth (strictly taken this is rarely fulfilled as ligament yielding and crack initiation/growth are usually superposed to one another), self-similarity of the load-displacement curves registered (minimum requirement from practical point of view). Self-similarity means that the F-x curves at different ligament lengths are overlapping by simple linear transformation. Details to the EWF method and its application to polymers, related blends and composites can be taken from recent reviews [1-4].

The extensive research on polymer nanocomposites extended also to their toughness determination. Unfortunately, for that purpose fracture mechanical approaches were seldom used, albeit these are the right tools to derive toughness parameters which are independent of the testing conditions. In addition, in many cases it remained unclear whether the observed change in the toughness can be traced to effects of nanofillers (i.e. dispersion characteristics, shape, specific surface data) or to nanofiller-caused

fundamental changes in the morphology. Note that the latter effect is the most severe for semi-crystalline thermoplastics generating alterations in polymorphism, crystallinity, lamellar characteristics, tie molecule density etc. [5]. Many research works devoted to the EWF testing of polymer nanocomposites disregarded morphology changes or clearly violated the above listed application criteria, even the less strict one, viz. the self-similarity of the load-displacement traces. This was pinpointed recently in a review [4].

According to the authors' standpoint in order to shed light on how nanofillers affect the toughness, assessed by the EWF approach, the following strategy should be followed: i) select polymer matrices which meet the EWF requirements, ii) choose nanofillers which can be homogeneously distributed, and iii) use nanofillers which have marginal impact on the morphology of the matrix. By this way one can get a clearer picture on where the change in the toughness of polymeric nanocomposites originates from.

It has been underlined earlier that "EWF-suitable" matrices are amorphous copolyesters [6] and semi-crystalline polypropylene copolymers [7-8]. The range of the "EWF-suitable" semi-crystalline polymers was recently extended by poly(ε-caprolactone) (PCL). This material fulfilled all the EWF prerequisites in neat [9], blend [10] and filled (microparticles such as hydroxyapatite [11] or different types of calcium-carbonate [12]) forms, as well. The only drawback of PCL is that the melting temperature of its crystals is close to room temperature, thus the room temperature storage ("annealing") may be accompanied with morphology changes. This, however, can be circumvented by testing well characterized specimens with the same "prehistory". The latter term means that the time interval between preparation and testing, along with the storage conditions, should be the same for the samples to be compared.

The possible range of nanofillers having marginal impact on the morphology in semicrystalline polymers is quite limited. Graphenes, carbon nanotubes, organoclays usually strongly affect the crystalline structure [5]. Moreover, no homogeneous filler distribution can be achieved via conventional melt compounding techniques. There is, however, some chance not to influence the morphology and to achieve fine and homogenous dispersion of nanoparticles. Wang et al. [13] reported that TiO_2 nanoparticles, in both neat and surface treated forms, had no significant effect on the crystalline structure. Their effect was restricted to the matrix crystallinity. The silane surface treatment of TiO_2 turned to be beneficial in respect to the dispersion of the corresponding nanoparticles in PCL.

Boehmite alumina (BA) with the composition of AlO(OH) seems to be also suitable nanofillers to meet the above listed requirements. BA could be well dispersed in polypropylene [14] and polyethylene [15, 16] - even without any surface treatment - and had a marginal effect on the morphology of the related semicrystalline matrices. However, BA was not yet incorporated in PCL.

Accordingly, the present work was focused to study the structure-toughness relationship in PCL/BA nanocomposites containing 5 and 10 wt% BA. To check whether the dispersion of BA is influenced by its

surface treatment, BA nanoparticles with octylsilane and alkylbenzene sulphonic acid treatments were also used. Recall that this work fits into the strategy to differentiate between dispersion- and morphology-related effects of nanoparticles on the toughness of nanocomposites.

2. EXPERIMENTAL

Materials and specimen preparation

The PCL used in this study was a commercially available material (Capa^{TM} 6500), procured by Perstorp UK Ltd. (Warrington, UK), with a nominal number average molecular weight of 50 kDa.

As nanofiller synthetic Disperal$^{®}$40 boehmite of Sasol GmbH (Hamburg, Germany) served. It has surface area of ~100 m^2/g and primary crystallite size of ~40 nm. BA was used in pristine (BA), and in surface treated forms. The latter occurred by octylsilane (BA-OS) and by C10–C13 alkylbenzene sulphonic acid (BA-OS2), respectively. BA was incorporated in 5 and 10 wt%, while the surface modified BAs only in 5 wt% in PCL.

Samples were prepared by melt mixing using a Berstorff co-rotating twin-screw extruder (ZE-40, Berstorff, Hannover, Germany) followed by granulation. The barrel temperatures from the hoper to die were 80, 80, 85, 85, 88, 88, 90, 90°C, the screw rotated at 60 rpm and the melt passed through the extruder in ca. 80 s. Sheets with a mean thickness of 0.8 mm were produced by compression molding from the granules using a P.H.I. press (Pasadena Hydraulics Inc., El Monte, CA, USA). The granules of PCL and PCL/BA were dried over night at 60°C prior to compression molding. The temperature of the latter agreed with that of the mixing (90°C) and the pressure was set for 2 MPa. After 15 min holding time the press was cooled by water.

For the tensile tests type 1BA specimens according to ISO 527-2:1999 were cut off the sheets. The EWF testing was performed on DENT specimens having a width (W) of 40 mm and length of 80 mm (clamped length 40 mm), respectively.

Dispersion of the BA nanoparticles

The dispersion of the BA particles was studied by inspecting the surface of cryofractured specimens in scanning electron microscope (SEM). Specimens, after immersion in liquid nitrogen for 5 min, were broken by immersed in liquid nitrogen for 5 min and after freezing they were impact broken. Scanning electron microscopic images were taken of the cryofractured surface of the specimens by JEOL 6380LA (JEOL Ltd., Tokyo, Japan) instrument after coating with an Au/Pd alloy.

Melting and crystallization behavior of the nanocomposites

Differential scanning calorimetry (DSC) was carried out on the samples by a TA Instruments Q2000 (TA Instruments, New Castle, DE, USA) DSC. The purge gas was nitrogen (25 ml/min), while liquid nitrogen was used for the cooling. The measurements were performed between -80 and 120°C with a heating and cooling rate of 10 °C/min. The results were evaluated according to ISO 11357-3 standard. The crystallinity of the samples (X) was calculated after normalizing with nominal polymer weight fraction and by taking the enthalpy of fusion of the 100% crystalline polymer as ΔH_o= 142.5 J/g [17].

Wide angle X-ray scattering (WAXD)

To check possible effects of BA on the crystalline structure of PCL WAXD measurements were performed. WAXD patterns of the polymer samples were recorded on a Phillips (PANalytical, Almelo, The Netherlands) X-ray diffractometer using a Cu K_α (λ = 0.154 nm) radiation source (45 kV and 40 mA). Data were collected in the scatter range of 2Θ = 5 to 40° with a step size of 0.02°.

Dynamic mechanical analysis (DMA)

Dynamic mechanical analysis of the polymer sheets was performed on a DMA Q800 (TA Instruments, New Castle, DE, USA) dynamic mechanical analyzer in strain controlled tension mode using a frequency of 1 Hz, an amplitude of 15 μm and a force track of 120%. The properties were measured between -80°C and 60°C with a heating rate of 3°C/min.

Mechanical and EWF testing of the nanocomposites

The tensile and fracture tests were performed at ambient conditions (24±0.5°C, RH=40±5%) on a Zwick Z020 (Zwick GmbH, Ulm, Germany) universal testing machine. The crosshead speed was set to 10 mm/min, the displacement values (x) were calculated from crosshead travel, while the load (F) was recorded by a 20 kN cell. For the determination of tensile properties five dumb-bell specimens were tested for each material. For the linear regression of EWF data at least 20 specimens were used. The validity of EWF method was confirmed by:

- the self-similarity of load-displacement curves,
- a check on the ligament yielding – method described in ref [18],
- a lower ligament limit (L=5 mm), which ensures quasi plane-stress conditions and steady-state crack propagation; determined as outlined in our previous paper [19],
- a confined plastic zone, which was ensured by the condition $L< x_p$, where x_p is the estimated size of the plastic zone based on Cotterell's study [20]. The other generally used criteria (i.e. $L<w/3$) seems to be too conservative, therefore L=18 mm was used as the upper ligament length limit.

3. RESULTS AND DISCUSSION

BA dispersion

Figure 2 confirms on high magnification SEM pictures that the BA was finely and homogenously dispersed in the PCL matrix. The mean particle size is at about 120 nm which is threefold of the primary crystallite size (cf. Experimental). Further, the surface treatment used did not affect considerably the dispersion of the BA nanoparticles. This finding confirms that BA can be easily and well dispersed, in fact, also in PCL.

Figure 2: SEM pictures taken from the fracture surfaces of PCL/BA nanocomposites. Designations: (a) BA in 5 wt%, (b) BA-OS in 5 wt%, (c) BA-OS2 in 5 wt% and (d) BA in 10 wt%

Melting and crystallization of PCL/BA

Table 1 summarizes the DSC results derived from the 1st heating, cooling and 2nd heating cycles, respectively. One can notice that the melting and related crystalline content data did not change with the type and amount of BA. On the other hand, BA worked as nucleating agent for PCL because both the onset and peak temperatures of the crystallization exotherms were shifted toward slightly higher temperatures.

Table 1: Melting and crystallization characteristics of the PCL and PCL/BA nanocomposites derived from DSC tests. Designations: T_{on} – onset of melting or crystallization, T_{mp} – melting peak temperature, T_{cp} – crystallization peak temperature. Note: the crystallinity (X) is normalized by the nominal filler amount.

	Filler type	-	BA	BA-OS	BA-OS2	BA
	Filler amount [wt%]	0	5	5	5	10
1st heating	T_{on} [°C]	57.0	58.3	59.5	57.1	60.6
	T_{mp} [°C]	61.1	65.4	67.7	65.4	66.4
	X [%]	56	60	59	59	59
cooling	T_{on} [°C]	33.9	39.5	38.2	32.5	40.3
	T_{cp} [°C]	32.2	37.5	36.4	29.5	37.8
	X [%]	40	47	46	47	46

2nd heating	T_{on} [°C]	54.3	54.1	54.4	54.0	53.6
	T_{mp} [°C]	56.6	58.7	59.0	58.4	58.5
	X [%]	47	53	50	51	50

Results in Table 1 suggest that the BA nanoparticles increase the crystallinity (between 3 and 7% depending whether results from melting or crystallization considered). On the other hand, the related change is less than 4% in the 1st heating representing the stage of the tested specimens. Moreover, the WAXD patterns (Figure 3) indicated that practically no change occurred in the crystalline fine structure of PCL owing to BA incorporation.

Figure 3: Wide angle X-ray diffractograms of PCL and PCL/BA nanocomposites. Note: the curves are shifted vertically

Dynamic mechanical analysis (DMA)

Figure 4a and b show the storage (*E'*) and loss moduli (*E''*) as a function of the temperature (*T*) for PCL and its BA nanocomposites.

Figure 4: DMA traces in form of (a) *E'* vs. *T*, and (b) *E''* vs. *T* curves for the PCL and PCL/BA nanocomposites

One can notice that BA incorporation only slightly increased the glassy (~10%) and more markedly the rubbery modulus of PCL (>20%) – the related data are summarized in Table 2. This is characteristic for "non-reinforcing" fillers which have no strong adhesion toward the matrix and low aspect ratio. The latter is the case with our BA particles as already indicated by the SEM pictures in Figure 2. The glass transition temperature (T_g) was not influenced significantly by filler content and type either, which suggests that there is no significant interaction on molecular level between the nanofiller and PCL macromolecules. The DSC and DMA results confirm that the BAs meet our selection criteria: good dispersability and less effect of on the morphology of the matrix.

Table 2: Glassy and rubbery moduli and T_g data for the PCL and PCL/BA nanocomposites. Notes: glassy and rubbery moduli were read at -70 and 23 °C, respectively, while the T_g was read as the peak temperature of the *E''* vs. *T* curve.

Filler type	Filler amount	E' [GPa]	E' [GPa]	T_g [°C]

	[wt%]	T=-70°C	T=23°C	
-	0	3.20	0.46	-54.8
BA	5	3.49	0.60	-54.4
BA-OS	5	3.45	0.56	-54.7
BA-OS2	5	3.56	0.58	-54.9
BA	10	3.50	0.60	-52.7

Tensile mechanical and EWF results

The tensile mechanical test results are summarized in Table 3. The corresponding data indicate that 5 wt% BA incorporation increased the modulus (<17%, except for BA-OS2 where it was almost 40%), did not affect the yield strength, and slightly reduced the yield strain (<7%, except for BA-OS2 where it was more than 40%). There was a big change in ductility of PCL/BA-OS2 also in respect to the elongation at break. This suggests that either the molecular weight of PCL was reduced by sulphonic acid compound or the latter improved the adhesion between the PCL and BA-OS2, or both processes took place. Prominent reduction in the molecular weight should be associated with enhancement in the crystallinity [23]. This was, however, not the case – cf. Table 1. Increment in the tensile elastic modulus and strong reduction in the elongation at yield and break data, being characteristic for "reinforcing" fillers, support the hypothesis on the improved adhesion. The big change in the ductility should be discernible in the *F-x* curves of the DENT specimens. Especially their post-yield necking/tearing sections should be affected, namely markedly reduced.

Table 3: Elastic modulus (E), yield strength (σ_Y), yield strain (ε_Y) and elongation at break (ε_B) of PCL and its BA nanocomposites

Filler type	Filler amount [wt%]	σ_Y [MPa]	ε_Y [%]	ε_B [%]	E [MPa]
-	0	18.1±0.4	15.2±1.1	>400	297±9
BA	5	18.4±0.5	14.8±1.1	>400	340±17
BA-OS	5	18.3±0.3	14.2±1.0	>400	347±10
BA-OS2	5	18.7±0.9	8.4±2.1	22±18	418±70
BA	10	20.4±0.2	12.3±1.2	>400	433±20

Figure 5 shows the F-x traces of the DEN-T specimens as a function of their ligament length. The neat PCL completely meet the often neglected EWF prerequisite, i.e. full ligament yielding prior to crack formation. This is well resolved by the sudden load drops in the traces in Figure 5a [6]. The "self-

similarity" of the *F-x* traces is also obvious in this Figure. Incorporation of BA in 5 wt% in PCL affects the ligament yielding which is not instantaneous (i.e. drop like) any more. Nonetheless, the *F-x* curves remain self-similar with each other further on (cf. Figure 5b). Delayed yielding and necking becomes even more prominent with increasing amount of BA (cf. Figure 5c), which can be explained by the higher yield strength of the material. Such delayed yielding has been found for other semi-crystalline polymers, such as syndiotactic polypropylene [4,21]. Octylsilane (OS) surface treatment of BA has only a marginal effect on the *F-x* behavior when comparing the nanocomposites with 5 wt% nanofiller contents (cf. Figure 5b and 5d). By contrast, the *F-x* traces did not even meet the self-similarity criterion after sulphonic acid treatment of BA (OS2) – cf. Figure 5e. Accordingly, for the latter system the EWF approach can hardly be adapted. On the other hand, the self-similarity still may hold for the yielding-related part (indicated by "y" in Figure 5a) of the F-x curves of PCL/BA-OS2. This can be clarified by the energy partitioning concept, described in detail in ref. [4].

Figure 5 F-x traces registered for the DEN-T specimens of (a) PCL, (b) PCL/BA 5 wt%, (c) PCL/BA 10 wt%, (d) PCL/BA-OS 5 wt% and (e) PCL/BA-OS2 5 wt%. Note: with increasing ligament length both the related load and displacement increase

For polymers with clear ligament yielding-related load drop Karger-Kocsis recommended the splitting of the *F-x* traces for yielding (y) and necking/tearing (n) related terms [6] as indicated also in Figure 5a. The mathematical treatise of this energy partitioning method is given by Equation (4):

$$w_f = w_{f,y} + w_{f,n} = \left(w_{e,y} + \beta w_{p,y} \cdot L\right) + \left(w_{e,n} + \beta w_{p,n} \cdot L\right) \quad (4)$$

where the terms with subscripts *y* and *n* are linked with the yielding and necking/tearing related processes, respectively. This kind of partitioning has been followed also in this work. The specific work of fracture and specific yielding-related work of fracture vs. ligament traces for the systems studied are summarized in Figure 6.

Figure 6 Specific work of fracture (w_f) and yielding related work of fracture (w_y) vs. ligament length (L) traces for the PCL and its nanocomposites. Designations: (a) PCL, (b) PCL/BA 5 wt%, (c) PCL/BA 10 wt%, (d) PCL/BA-OS 5 wt% and (e) PCL/BA-OS2 5 wt%.

As expected, the EWF approach is blurred for the PCL/BA-OS2 system. Therefore, this nanocomposite has been discarded from the EWF treatise; only the yielding-related fracture terms were calculated and given in Figure 6e. By contrast, the w_f vs. L traces for all other systems obeyed the linearity – cf. Table 4. Wong et al. [10] found similar values for w_e and slightly lower values for βw_p, in PCL-hydroxyapatite microcomposites. Nevertheless, it should be noted that the confidence bands of their measurements were not presented and the deviation of results could be rather high because of the small sample size (see the theory of linear regression or the paper of Pegoretti et al. [22]). Additionally, the number average molecular weight of the studied PCLs was not the same either, which also influences the w_e and βw_p parameters as it was shown in one of our previous studies [23].

At the first glance, there is a rather small difference in the basic EWF parameters (i.e. w_e, βw_p) for all other systems, especially when considering the related data within their 95% confidence limits. Based on the data in Table 4 one can state that the incorporation of BA did not affect the essential work of fracture markedly. The only exception in this respect may be the PCL/BA 5 wt% system. This finding suggests that the BA nanofillers (except the OS2 treated one) did not influence the molecular mobility and crystalline structure of the PCL matrix which is in line with the DSC, DMA and mechanical test results (cf. Tables 1-3). The resistance to crack propagation, reflected by the βw_p term, decreased in presence of the BA nanofiller. Interestingly, the amount of BA had no further effect on this term. This finding is in line with the designation of BA as "non-reinforcing" filler.

A deeper insight in the structure-toughness relationship is expected, however, when collating the yielding-related essential and non-essential EWF parameters, which are also incorporated in Table 4. Note that the yielding-related part of PCL with 5 wt% BA-OS2 was also analyzed by the above mentioned energy partitioning method (cf. Figure 6e). The yielding-related essential work of fracture, $w_{e,y}$, decreased with increasing amount of BA compared to that of the PCL. The related reduction was slightly smaller for the OS-treated BA than for the neat one determined at similar regression coefficients. Reduction of $w_{e,y}$ is not surprising as nanofillers, acting as "non-reinforcing" particles, trigger matrix/filler debonding which affects the yielding. Comparing the $w_{e,y}$ and yield strain (ε_Y) in Tables 4 and 3, respectively, one can observe that they run parallel. Recall that the yield strength (σ_Y) did not change due to BA filling or modification (cf. Table 3), The change in the yielding-related essential work of fracture term can be correlated with the product of ε_Y *and* σ_Y from the tensile tests. On the other hand, the yielding related non-essential work of fracture term ($\beta w_{p,y}$) increased by BA filling and reflected also changes in the BA surface modification. This can be attributed to beneficial effects of debonding. This argument is supported by the fact that the related term of PCL-BA OS2, for which a better matrix/filler adhesion was concluded, is lower than for the other nanocomposites.

Table 4 EWF parameters determined for the PCL and its BA nanocomposites. Note: for parameters the 95% confidence limits are indicated

Filler type	Filler amount [wt%]	w_e [kJ/m^2]	βw_p [MJ/m^3]	R^2 [-]	$w_{e,y}$ [kJ/m^2]	$\beta w_{p,y}$ [MJ/m^3]	R^2 [-]
-	0	54.5±15.6	18.7±1.3	0.98	13.9±3.8	1.3±0.3	0.85
BA	5	70.4±15.2	15.6±1.4	0.97	6.7±3.2	2.1±0.3	0.93
BA-OS	5	56.9±17.2	16.4±1.5	0.96	7.2±2.7	2.2±0.2	0.94
BA-OS2	5	-	-	-	1.4±3.6	1.7±0.4	0.88
BA	10	55.5±16.6	15.7±1.4	0.96	3.2±3.1	2.2±0.3	0.93

CONCLUSION

In this work the effect of boehmite (BA) nanofillers on the morphology, mechanical and fracture mechanical properties of poly(ε-caprolactone) (PCL) was investigated. Boehmite was selected in order to achieve marginal changes in the crystalline phase and thus get a clear picture on effects caused by the nanoparticles themselves. For that purpose PCL/BA nanocomposites containing 5 and 10 wt% BA with and without surface treatments were prepared. BA particles were treated with octylsilane and alkylbenzene sulphonic acid.

The filler amount and surface treatment did not influence the filler dispersion considerably; the composites had homogeneously dispersed structure with small amount of agglomerates. Slight increase of crystallinity (~3%) and melting temperature (~4°C) was observed, and the crystallization temperatures also shifted to higher temperatures (~5°C). This was ascribed to the heterogeneous nucleating effect of nanofillers. Neither the filler amount nor the surface treatment resulted, however, in further changes.

The DMA results indicated that there is no molecular level interaction between the polymer and the filler – the T_g values remained unaltered. Marginal increase of rubbery and glass moduli were, however, observed. The yield strength and the elongation at break were nearly the same for the examined materials, except for the sulphonic acid treated BA filled composite, that one became more brittle than the others. The similar yield strength, elongation at break and storage moduli values indicated that BA acted as "non-reinforcing" filler. The elongation at yield slightly decreased and the tensile modulus increased with increasing filler content, because of the incorporation of rigid particles. Again, the surface treatment only affected the properties of sulphonic acid treated BA composites. For the latter better matrix/filler interfacial adhesion was concluded, which resulted in a stiffer, less ductile material compared to the others.

The essential work of fracture (EWF) method was applicable for the composites except for the sulphonic acid treated BA/PCL composite, where the stable crack propagation and the self-similarity of load-displacement curves were absent. The essential work of fracture (w_e) remained also unaltered when considering the 95% confidence limits, while the plastic work of fracture (βw_p) decreased with increasing filler content. This also underlines that a "non-reinforcing" filler will not improve the essential work of fracture until the crystalline morphology remains the same. On the other hand, the non-essential (plastic) work decreased with increasing amount of BA. This was accompanied with a shrinking plastic zone. The curve partitioning of load-displacement curves of EWF tests has revealed, that the yielding related work of fracture ($w_{e,y}$) decreased with increasing filler content and enhanced interfacial adhesion. This observation is in line with the changes observed for the tensile yield data of the PCL/BA nanocomposites, i.e. marginal change in the yield strength and decreasing elongation at yield reflecting that BA was a non-reinforcing filler.

ACKNOWLEDGEMENTS

This work was supported by the Hungarian-Italian Bilateral program "On the toughness of thermoplastic nanocomposites as studied by the essential work of fracture (EWF) approach" (Project-ID: TÉT-10-1-2011-0218), is connected to the scientific program of the "Development of quality-oriented and harmonized R+D+I strategy and functional model at BME" (Project ID: TÁMOP-4.2.1/B-09/1/KMR-2010-0002) and the "Talent care and cultivation in the scientific workshops of BME" (Project ID: TÁMOP - 4.2.2.B-10/1-2010-0009) projects.

References

[1] Mai, Y.-W.; Wong, S.-C.; Chen X.-H. in "Polymer Blends: Formulations and Performance" (eds.: Paul, D.R. and Bucknall, C.B.), Wiley, New York, 2000, pp. 17-58.
[2] Williams, J.G.; Rink M. Engineering Fracture Mechanics 2007, **74**, 1009.
[3] Martinez, A. B.; Gamez-Perez, J.; Sanchez-Soto, M.; Velasco, J.I.; Santana, O.O.; Maspoch, M. Ll. Engineering Failure Analysis 2009, **16**, 2604.
[4] Bárány, T.; Czigány, T.; Karger-Kocsis, J. Progress in Polymer Science 2010, **35**, 1257.
[5] Karger-Kocsis, J. in "Nano- and Micromechanics of Polymer Blends and Composites" (eds.: Karger-Kocsis, J. and Fakirov, S.), hanser, Munich, 2009, pp. 425-470
[6] Karger-Kocsis, J. Polymer Bulletin 1996, **37**, 119.
[7] Ferrer-Balas, D.; Maspoch, M. Ll.; Martinez, A. B.; Santana, O. O. Polymer Bulletin 1999, **42**, 101.
[8] Ferrer-Balas, D.; Maspoch, M. Ll.; Martinez, A. B.; Ching, E.; Li, R.K.Y.; Mai Y.-W. Polymer, 2001, **42**, 2665.
[9] Tuba, F.; Oláh, L.; Nagy, P. Journal of Materials Science 2011, **46**, 7901.
[10] Tuba, F.; Oláh, L.; Nagy, P. Engineering Fracture Mechanics 2011, **78**, 3123.
[11] Wong, S.-C.; Baji, A.; Gent A. N. Composites Part A: Applied Science and Manufacturing 2008, **39**, 579.
[12] Tuba, F.; Oláh, L.; Nagy, P. Journal of Applied Polymer Science 2011, **120**, 2587.

[13] Wang, G.; Chen, G.; Wei, Z.; Yu, T.; Liu, L.; Wang, P.; Chang, Y.; Qi, M. Journal of Applied Polymer Science 2012, **125**, 3871.
[14] Streller, R. C.; Thomann, R.; Torno, O.; Mülhaupt, R. Macromolecular Materials and Engineering 2008, **293**, 218.
[15] Khumalo, V. M.; Karger-Kocsis, J.; Thomann, R. Express Polymer Letters 2010, **4**, 264.
[16] Khumalo, V. M.; Karger-Kocsis, J.; Thomann, R. Journal of Materials Science 2011, **46**, 422.
[17] Crescenzi, V.; Manzini, G.; Calzolari, G.; Borri, C. European Polymer Journal 1972, **8**, 449.
[18] Tuba, F.; Oláh, L.; Nagy, P. Engineering Fracture Mechanics (in press)
[19] Tuba, F.; Oláh, L.; Nagy, P. Journal of Materials Science 2012, **47**, 2228.
[20] Cotterell, B., Pardoen, T.; Atkins, A. G. Engineering Fracture Mechanics 2005, **72**, 827.
[21] Karger-Kocsis, J.; Bárány, T. Polymer Engineering & Science 2002, **42**, 1410.
[22] Pegoretti, A.; Castellani, L.; Franchini, L.; Mariani, P.; Penati, A. Engineering Fracture Mechanics 2009, **76**, 2788.
[23] Tuba, F.; Oláh, L.; Nagy, P. unpublished results (2012)

FIGURES

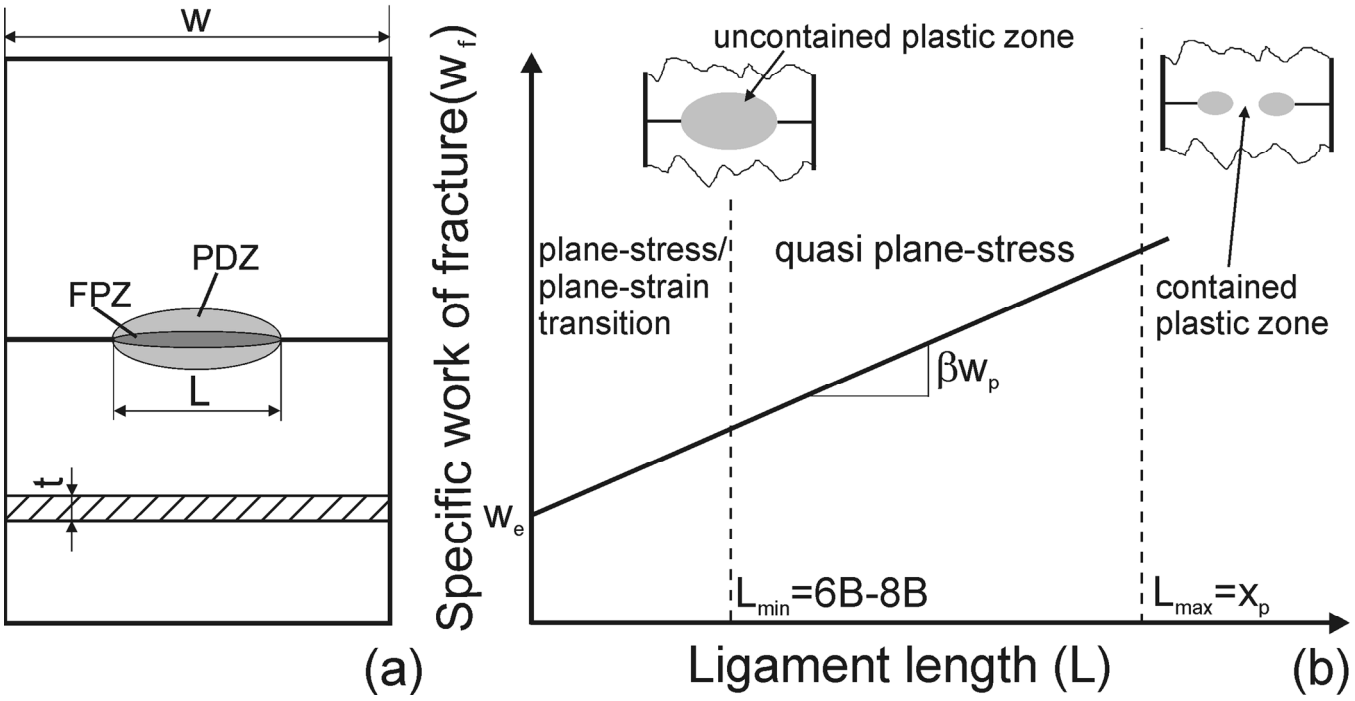

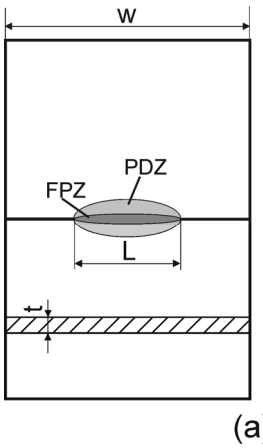

(a)

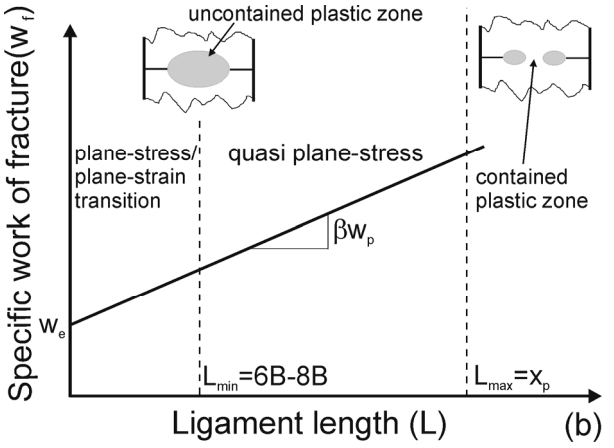
uncontained plastic zone
plane-stress/
plane-strain
transition
quasi plane-stress
contained
plastic zone
βw_p
w_e
L_min=6B-8B
L_max=x_p
Specific work of fracture(w_f)
Ligament length (L)
(b)

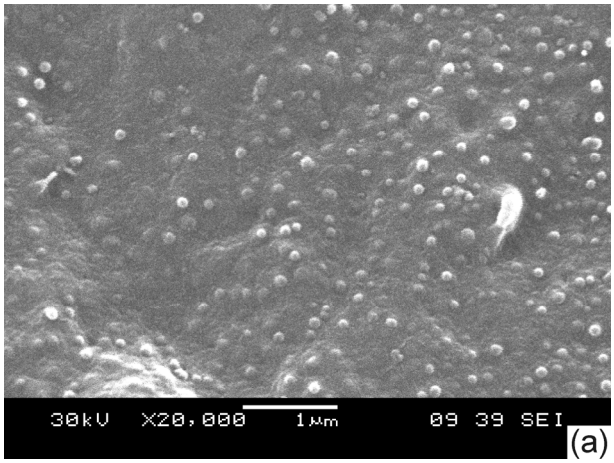
30kV X20,000 1μm 09 39 SEI
(a)

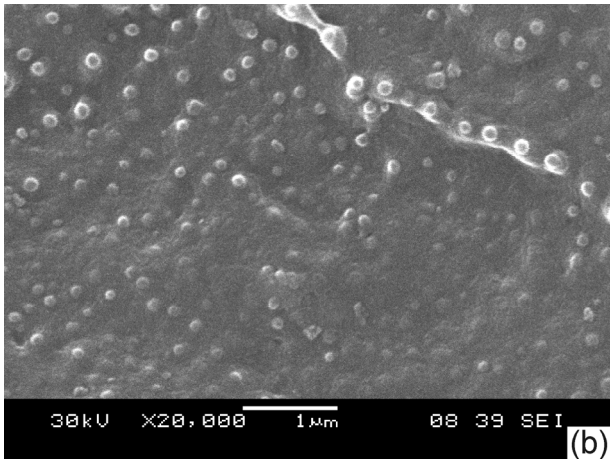
30kV X20,000 1μm 08 39 SEI
(b)

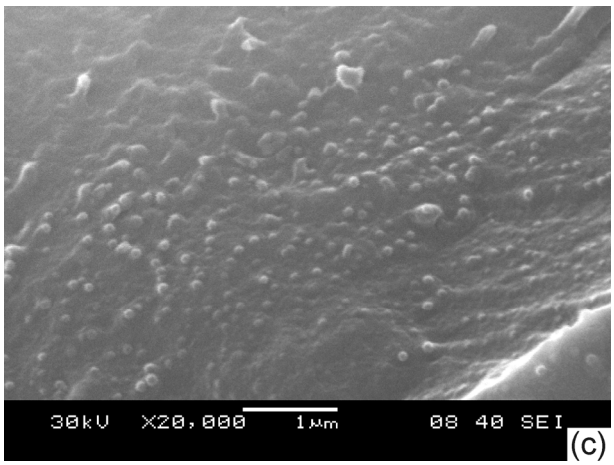
30kV X20,000 1μm 08 40 SEI
(c)

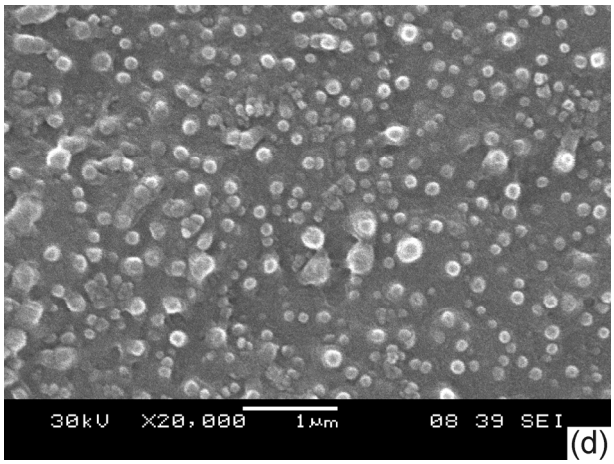
30kV X20,000 1μm 08 39 SEI
(d)

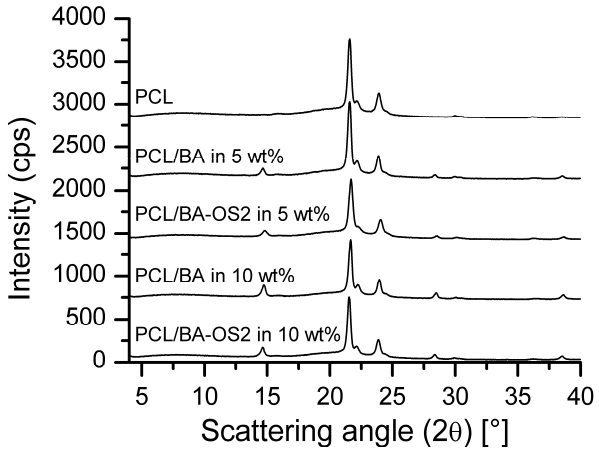
Intensity (cps)
4000
3500
3000
2500
2000
1500
1000
500
0
PCL
PCL/BA in 5 wt%
PCL/BA-OS2 in 5 wt%
PCL/BA in 10 wt%
PCL/BA-OS2 in 10 wt%
5
10
15
20
25
30
35
40
Scattering angle (2θ) [°]

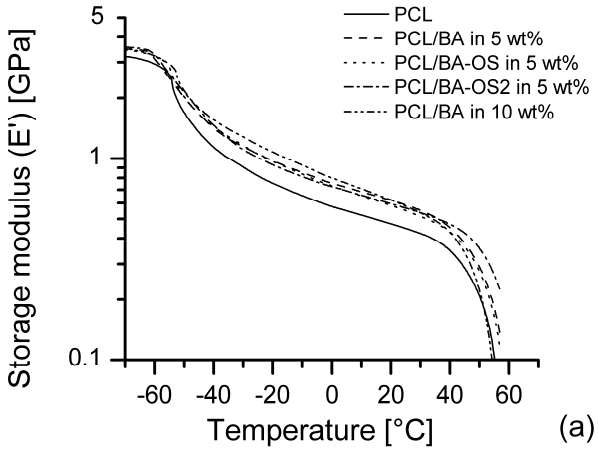
Storage modulus (E') [GPa]
5
1
0.1
PCL
PCL/BA in 5 wt%
PCL/BA-OS in 5 wt%
PCL/BA-OS2 in 5 wt%
PCL/BA in 10 wt%
-60
-40
-20
0
20
40
60
Temperature [°C]
(a)

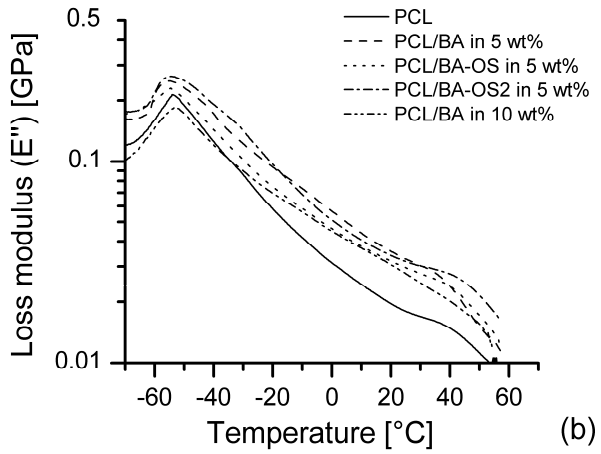
PCL
PCL/BA in 5 wt%
PCL/BA-OS in 5 wt%
PCL/BA-OS2 in 5 wt%
PCL/BA in 10 wt%
Loss modulus (E'') [GPa]
0.5
0.1
0.01
-60 -40 -20 0 20 40 60
Temperature [°C]
(b)

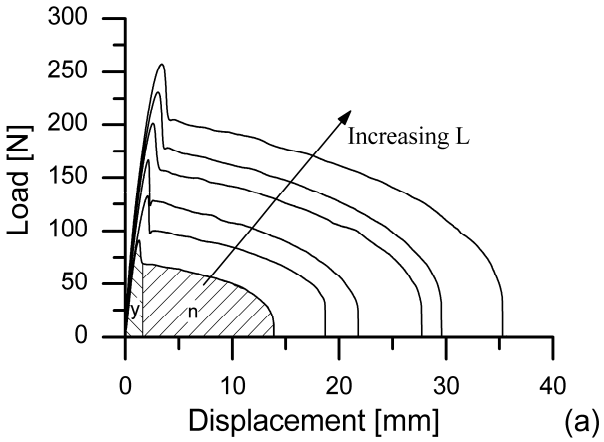
Load [N]
300
250
200
150
100
50
0
Increasing L
y
n
0 10 20 30 40
Displacement [mm]
(a)

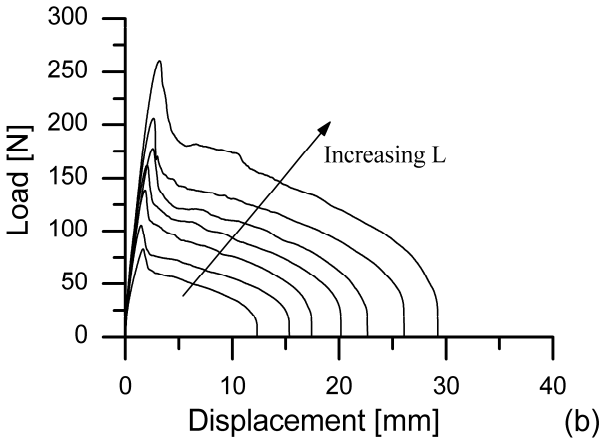
Load [N]
300
250
200
150
100
50
0
Increasing L
0 10 20 30 40
Displacement [mm]
(b)

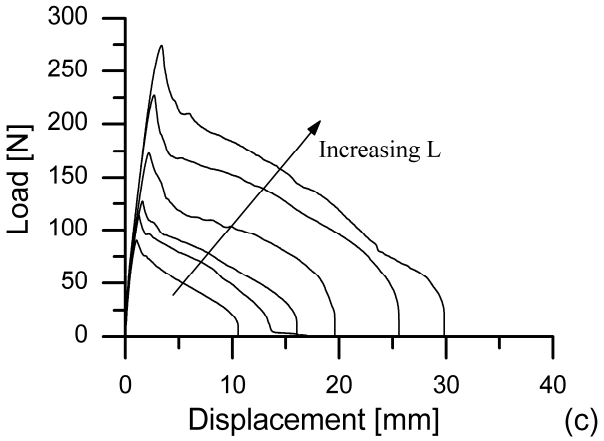
Load [N]
Displacement [mm]
Increasing L
(c)

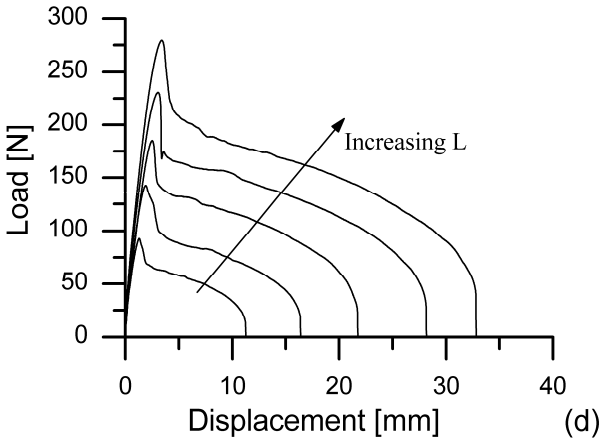
Load [N]
Displacement [mm]
Increasing L
(d)

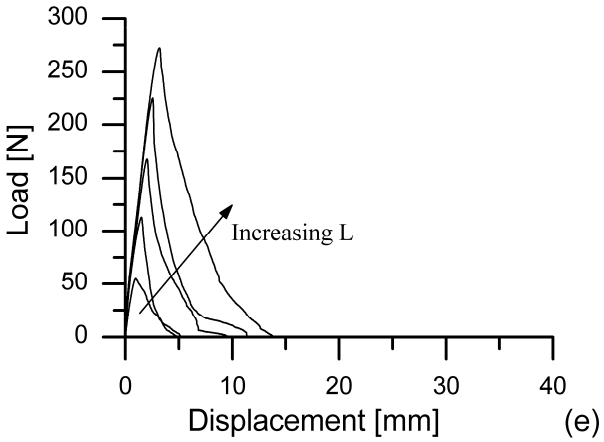
Load [N]
Displacement [mm]
Increasing L
(e)

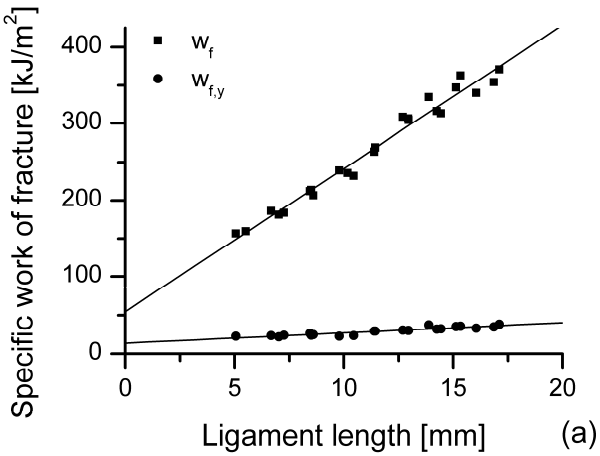
Specific work of fracture [kJ/m²]
w_f
w_f,y
0
100
200
300
400
0
5
10
15
20
Ligament length [mm]
(a)

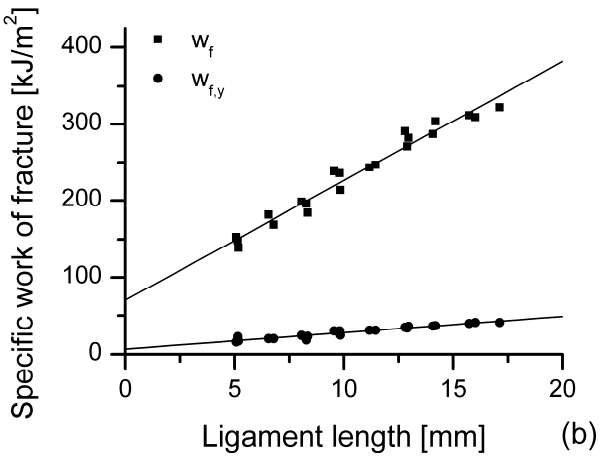
Specific work of fracture [kJ/m²]
w_f
w_f,y
0
100
200
300
400
0
5
10
15
20
Ligament length [mm]
(b)

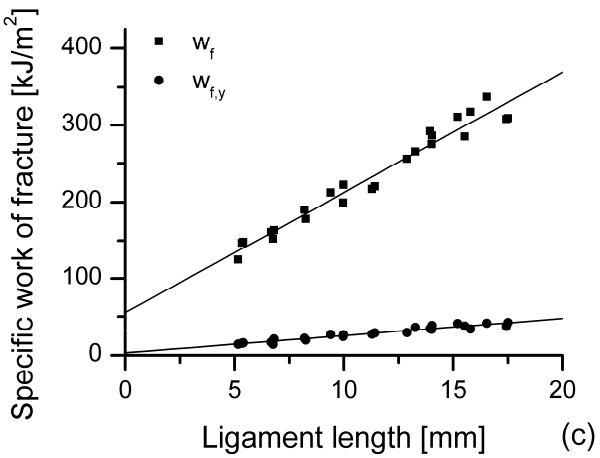
Specific work of fracture [kJ/m²]
w_f
w_f,y
0
100
200
300
400
0
5
10
15
20
Ligament length [mm]
(c)

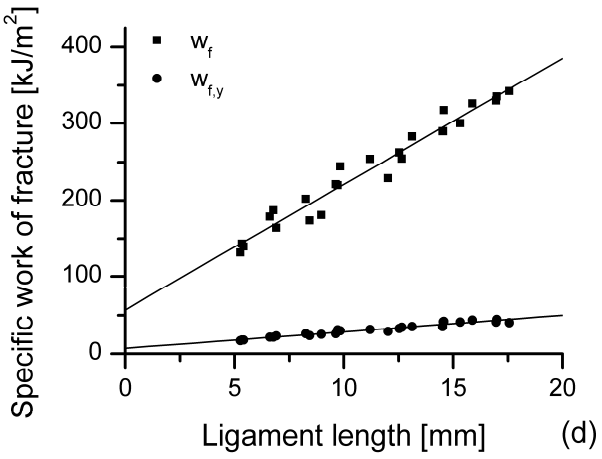
Specific work of fracture [kJ/m²]
w_f
w_f,y
400
300
200
100
0
0
5
10
15
20
Ligament length [mm]
(d)

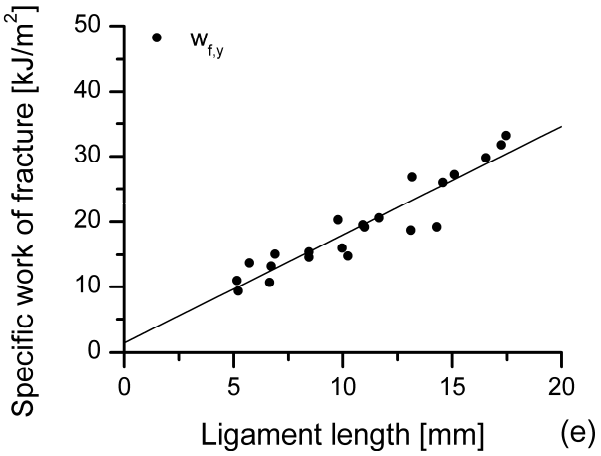
Specific work of fracture [kJ/m²]
w_f,y
50
40
30
20
10
0
0
5
10
15
20
Ligament length [mm]
(e)